Phenotypic and microRNA characterization of the neglected CD24+ cell population in MCF-7 breast cancer 3-dimensional spheroid culture

Lily Boo[a], Swee Keong Yeap[b], Norlaily Mohd Ali[a], Wan Yong Ho[c], Huynh Ky[d], Dilan Amila Satharasinghe[e,f], Woan Charn Liew[e], Sheau Wei Tan[e], Mong-Lien Wang[g,h], Soon Keng Cheong[a], Han Kiat Ong[a,*]

[a]Department of Preclinical Sciences, Faculty of Medicine and Health Sciences, Universiti Tunku Abdul Rahman, Cheras, Malaysia; [b]China-ASEAN College of Marine Sciences, Xiamen University Malaysia Campus, Jalan Sunsuria, Bandar Sunsuria, Sepang, Selangor, Malaysia; [c]Division of Biomedical Sciences, Faculty of Medicine and Health Sciences, University of Nottingham (Malaysia Campus), Semenyih, Malaysia; [d]Department of Agriculture Genetics and Breeding, College of Agriculture and Applied Biology, Can Tho University, Vietnam; [e]Laboratory of Vaccine and Immunotherapeutics, Institute of Bioscience, Universiti Putra Malaysia, Serdang, Malaysia; [f]Department of Basic Veterinary Sciences, Faculty of Veterinary Medicine and Animal Science, University of Peradeniya, Sri Lanka; [g]Division of Basic Research, Department of Medical Research, Taipei Veterans General Hospital, Taipei, Taiwan, ROC; [h]Institute of Food Safety and Health Risk Assessment, National Yang-Ming University, Taipei, Taiwan, ROC

Abstract

Background: In vitro 3-dimensional (3D) spheroid culture has been widely used as model to enrich $CD44^+CD24^{dim/-}$ cancer stem cells (CSC) with high aldehyde dehydrogenase 1 (ALDH1) activity. Although $CD24^+$ subpopulation was known to be present in 3D spheroids and may influence cancer drug therapies, its characteristics and CSC properties were not well defined.

Methods: In this study, $CD24^+$ population from the Michigan Cancer Foundation-7 (MCF-7) spheroid was sorted and subjected to spheroid formation test, stem cell markers immunofluorescence, invasion and migration test, as well as microRNA expression profiling.

Results: Sorted MCF-7 $CD24^+$ cells from primary spheroids were able to reform its 3D spheroid shape after 7 days in nonadherent culture conditions. In contrast to the primary spheroids, the expression of SOX-2, CD44, CD49f, and Nanog was dim in MCF-7 $CD24^+$ cells. Remarkably, MCF-7 $CD24^+$ cells were found to show high expression of ALDH1 protein which may have resulted in these cells exhibiting higher resistance against doxorubicin and cisplatin when compared with that of the parental cells. Moreover, microRNA profiling has shown that the absence of CSC properties was consistent with the downregulation of major CSCs-related pathways including Hedgehog, wingless-related integration site (Wnt), and microtubule associated protein kinase (MAPK) signaling pathways. However, the upregulated pathways such as adherens junctions, focal adhesion, and tight junction suggest that $CD24^+$ cells were probably at an epithelial-like state of cell transition.

Conclusion: In conclusion, neglected $CD24^+$ cells in MCF-7 spheroid did not exhibit typical breast CSCs properties. The presence of miRNAs and their analyzed pathways suggested that these cells could be a distinct intermediate cell state in breast CSCs.

Keywords: Doxorubicin; Hedgehog; MicroRNA

1. INTRODUCTION

Cancer cells were normally found with distinct phenotypes which are associated with specific functional properties. For the subpopulation of stem-like cancer cells, the distinct phenotypes commonly observed are their tumor-initiating ability, tumor progression, and drug resistance capacity which often results in tumor relapse.[1] This stem-like cancer cells were normally identified with $CD44^+/CD24^{-/low}$ phenotypes particularly in the case of breast cancer.[2] Breast cancer is still the most commonly diagnosed cancer, which contributed to the second highest number of cancer-associated death in females.[3] Breast cancer cell lines have been widely used as an in vitro model to represent in vivo breast cancer particularly in the evaluation of stem-like cancer cells subpopulation.[2,4] Among the breast cancer cell lines, Michigan Cancer Foundation-7 (MCF-7) is most widely used in research and publishing.[4] In addition, the drug-resistant and stem-like properties of MCF-7 were previously evaluated in detail using spheroid culture method.[5,6]

Breast cancer stem cells (CSCs) were found with low adherent characteristic, sustainable in serum-free media and capable of forming 3-dimensional spheroids.[7,8] In addition, MCF-7 cells that were cultured in 3-dimensional spheroid via aggregation method recorded a higher level of $CD44^+CD24^-$ population compared with that of the monolayer cultured cells. Furthermore, MCF-7 spheroids that expressed high levels of aldehyde dehydrogenase (ALDH) activity also showed resistance against most of the breast cancer chemotherapeutic drugs.[5] Thus, spheroid culture has been widely used as a model for drug discovery studies against CSC.[2,7] Although a much higher percentage of

*Address correspondence: Dr. Han Kiat Ong, Faculty of Medicine and Health Sciences, Universiti Tunku Abdul Rahman, 43000 Cheras, Malaysia. E-mail address: onghk@utar.edu.my (A.K. Ong).

Conflicts of interest: The authors declare that they have no conflicts of interest related to the subject matter or materials discussed in this article.

Journal of Chinese Medical Association. (2020) 83: 67-76.

Received August 31, 2019; accepted September 27, 2019.

doi: 10.1097/JCMA.0000000000000226.

stem-like cell population exists in spheroid-derived enrichment culture, the presence of the $CD24^+$ non–stem-like subpopulation warrants further attention as previous studies have shown the dynamic interconversion of these two subpopulations of cells in breast CSC.[1,9,10] Thus, understanding the interaction between the subpopulation of cells that coexist in the spheroid could facilitate the development of more effective and targeted therapies. To date, the stem-like $CD44^+CD24^-$ population of breast cancer has been well documented,[11–13] but the biological and molecular characteristics of $CD24^+$ subpopulation, which is commonly accepted as non–stem-like subpopulation,[1,5] are still lacking. Therefore, this study aims to sort and characterize the $CD24^+$ subpopulation of cells from MCF-7 spheroids.

2. METHODS

2.1. Cell culture

Established estrogen-dependent human breast adenocarcinoma cell line MCF-7 American Type Culture Collection (ATCC) HTB-22 was obtained from American Type Culture Collection (ATCC, University Boulevard Manassas, VA 20110 USA). The cells were grown and maintained in monolayer condition in RPMI-1640 medium supplemented with 10% fetal bovine serum and 2 mM L-glutamine at 37°C with humidified 5% CO_2.

2.2. Spheroid formation

MCF-7 spheroid cells were generated using an agar overlay technique in accordance to previously published work.[5] Briefly, MCF-7 monolayer cells were harvested by trypsinization, and the dissociated single cells were seeded in a 96-well tissue culture wells coated with 1% agarose at seeding density of 5×10^4 cells per well. All the wells were supplemented with serum-free medium and subjected to centrifugal force at 2000 rpm for 5 minutes to facilitate the spheroid formation. The plates were then cultured in a 37°C humidified cell culture incubator supplemented with 5% CO_2 atmosphere.

2.3. Cell sorting and CD24 secondary spheroid formation

For the cell sorting, the spheroid cells were treated with Accutase (GIBCO, Thermo Fisher Scientific, Third Avenue Waltham, MA, USA) before filtered through a 70 µm cell strainer (BD Biosciences, Franklin Lakes, New Jersey, USA) to ensure a single-cell suspension. The supernatant were then centrifuged at 1800 rpm for 5 minutes and then washed in ice-cold 1× Phosphate-Buffered Saline (PBS). After wash, the cell pellet was resuspended in 100 µL buffer containing 1:100 diluted CD24-microbeads antibodies (Miltenyi Biotec, Bergisch Gladbach, Germany,) and further incubated at 4°C for 30 minutes. After the incubation, 3 mL of ice-cold 1× PBS was added to wash the cells before centrifugation at 2000 rpm for 5 minutes. The cell pellet was then resuspended in 3 mL of 1× PBS and transferred to the LS columns (Miltenyi Biotec) attached to a magnetic stand. The cells suspensions were allowed to eluted out through column by gravity flow, with a tube catching the CD24-negative, flowthrough, population. The column was then washed three times and removed from the magnet stand before transferred to a new tube. The CD24-positive cell population was then ejected by applying 3 mL of 1× PBS to the column with the help from the plunger. Cell count was performed to determine the percentage of cells with CD24-positive surface marker. The resulted MCF-7 spheroid-derived $CD24^+$ cell population was then regrown in serum-free medium using nonadherent plates to investigate on their spheroid formation ability. The medium was topped up on alternative days till spheroids were 14 days old before further downstream analysis. The formed spheroid cells were observed and photographed using an inverted microscope (Nikon, Tokyo, Japan).

2.4. Immunofluorescence staining

MCF-7 spheroid-derived $CD24^+$ cells and their parental counterparts were first fixed in 4% cold paraformaldehyde and blocked with 0.2% bovine serum albumin for 1 hour before antibodies staining. To minimize samples loss, spheroid cells were stained in a microcentrifuge tube and pelleted down at each washing step. For intracellular markers (Oct4, Sox2, and Nanog), the cells were permeabilized with 0.1% Triton-X for 10 minutes, whereas standard immunofluorescence staining protocol was applied for the rest of the surface markers antibodies staining. All the antibodies were purchased from Miltenyl Biotech. The specimens were counterstained with nuclear stain before the images were captured using a fluorescent microscope (Carl Zeiss, SMT GmbH, Germany).

2.5. ALDH detection assay

Aldehyde (ALDH) activity was analyzed using the Aldefluor kit (Stem Cell Technologies, Vancouver, BC, Canada) following the manufacturer's protocol. The disaggregated single cells were mixed with activated Aldefluor reagent, with and without diethylaminobenzaldehyde specific inhibitor and incubated at 37°C for 45 minutes. Next, tubes were centrifuged to remove the supernatant before suspension in 0.5 mL Aldefluor buffer on ice. For data acquisition of ALDH activity, flow cytometry was performed with a FACS Calibur Flow Cytometer (BD Biosciences, USA), and figures were analyzed using Cell Quest Pro software.

2.6. Wound healing, invasion, and migration assays

Parental and spheroid CD24-positive cells were grown to confluence in a 6-well plate. A line was drawn with a marker pen on the bottom of the plate. A scratch was made using a sterile 200-µL pipette tip through the cells moving perpendicular to the line drawn in the step before. The wells were then carefully rinsed to remove the detached cells. Images of the wound were captured using an inverted microscope at 6-, 12-, and 24-hour time intervals. The areas of the wounds at different time points were analyzed using Image J software to quantify the cell migration rate. For cell invasion and migration assays, both assays were performed using the transwell inserts of 8 µm pore size filter in a 24-well plate (BD, USA). A thin layer of Matrigel (BD) was coated onto the transwell inserts for the invasion assay. Cells were starved in serum-free medium, dissociated into single cells before seeded onto the transwell inserts and cultured for 72 hours. The inserts were then removed, fixed, and stained with crystal violet before the images were captured using an inverted microscope. To quantitate the percentage of invaded/migrated cells on the stained inserts, the dye was extracted using 30% acetic acid and the absorbance was measure at 590 nm. The experiments were performed in triplicates.

2.7. MTT drug sensitivity assay

Sensitivity of the sorted $CD24^+$ MCF-7 cells was tested using 3-(4,5-dimethylthiazol-2-yl)-2,5-diphenyl-tetrazolium bromide (MTT) assay (Boo et al,[5] 2016). Briefly, the sorted cells were seeded as monolayer with RPMI-1640 medium supplemented with 10% fetal bovine serum at 5×10^3 cells/well in 96 well plate for overnight. Then, the cells were treated with either cisplatin or doxorubicin at 2-fold serial dilution starting from the highest concentration of 30 µg/mL. Sorted $CD24^+$ cells that only cultured with media were served as untreated control. After 96 hours of incubation, 20 µL of MTT at 5 mg/mL was added to all well and further incubated for 4 hours. Then, the formazan crystals were dissolved with 100 µL of Dimethyl sulfoxide (DMSO), and the absorbance was recorded using microplate reader at 570 nm. Concentration of drug that reduced 50% of cell viability (IC_{50}) was determined from the dose-response curves.

2.8. miRNA next-generation transcriptomic sequencing

Total RNA with retention of miRNAs was isolated and subjected to small library preparation by using TruSeq Small RNA Sample Preparation Kit (Illumina, USA). Briefly, total RNAs from six samples (three from parental MCF-7 cells and three from MCF-7 spheroid-derived $CD24^+$) with 1×10^6 cells per sample were isolated using the miRNeasy kit (Exiqon, Denmark) in accordance to their manufacturer's guidelines. The concentration and purity of the extracted RNA were determined using optical density (OD) measurements before Qubit RNA assay kit, Agilent 2100 Bioanalyzer (Agilent Technologies, Santa Clara, California, USA). The integrity of the samples was checked using the Agilent 2100 Bioanalyzer. RNA samples with concentration >600 ng/μL and RNA integrity number (RIN) >8 were used for the library preparation. A total of 3 μg of total RNA per sample was ligated to 5′ and 3′ adaptors sequentially, transcribed to complementary DNA (cDNA), and followed by polymerase chain reaction (PCR) amplification with unique index sequences. The generated cDNA libraries were then assessed using HS-DNA chip (Agilent Technologies, USA). The miRNA fragments with a size between 145 and 160 bp were then excised from the 6% polyacrylamide gel electrophoresis (PAGE), purified, and eluted. All the final libraries were then measured, checked for their qualities, and pooled at a final concentration of 2 nM before sequenced in an Illumina HiSeq Run (Illumina, San Diego, California, USA).

2.9. Data analysis

CLC Genomics Workbench (Qiagen, Germantown, MD, USA) Version 7.0 was used to process the raw miRNA transcriptome reads. The software allows the data trimming, filtration of low reads, and cleaning up the contaminating reads. After the initial analysis, the read lengths were filtered with the cutoff length at 17 nucleotides and not more than 27 nucleotides. The trimmed sequences were then mapped to the known miRNA database (miRBase-19) and Ensembl human genome (Homo Sapiens GRCh 37.57). For determination of differential gene expression, the generated list of miRNAs between the parental and the spheroid-derived $CD24^+$ cells was then subjected to statistical analysis using Kal's Z-test and the resulting p values were corrected using Benjamini-Hochberg method. Only expression ratios of the expressed miRNAs between the samples with fold change >2 and p value <0.05 were considered to be statistically significant expression. To assess their relationships between the expressed miRNAs and their target genes, miRNA target genes interaction networks were performed using Cytoscape (Institute for Systems Biology, Seattle, WA, USA) version 3.30. Gene ontology (GO) analysis was also performed using Database for Annotation, Visualization and Integrated Discovery program at a significance level of 0.05. Enrichment analysis of the interactions between the predicted genes and pathways was also performed using the Kyoto Encyclopedia of Genes and Genomes (KEGG).

2.10. Quantitative PCR

A 100 ng of total RNA containing the miRNAs was polyadenylated before reverse transcribed into cDNA using the universal reverse transcription (RT) first-strand synthesis reaction (microRNA PCR Panel, Exiqon, Denmark). Each reaction was performed in a 1:1 diluted cDNA and the mastermix provided in the kit, prepared in a final volume of 10 μL. PCR reaction was performed in a CFX96 Touch Real-time thermal cycler (Bio-Rad Laboratories, Hercules, California, USA), with denaturation at 95°C for 10 minutes; followed by 40 cycles of 95°C, 10 seconds; and 60°C, 1 minute. The results were analyzed using the Bio-Rad CFX Manager (Bio-Rad Laboratories, USA). Relative miRNA expression levels were calculated by the comparative Ct values method and were normalized against internet reference miRNAs based on geNorm algorithms.

3. RESULTS

3.1. Sorting and spheroid formation test of $CD24^+$ MCF-7 cells

Approximately 2.54 ± 1.25% of cells (Fig. 1) from primary MCF-7 spheroid were sorted as $CD24^+$ cells and were then

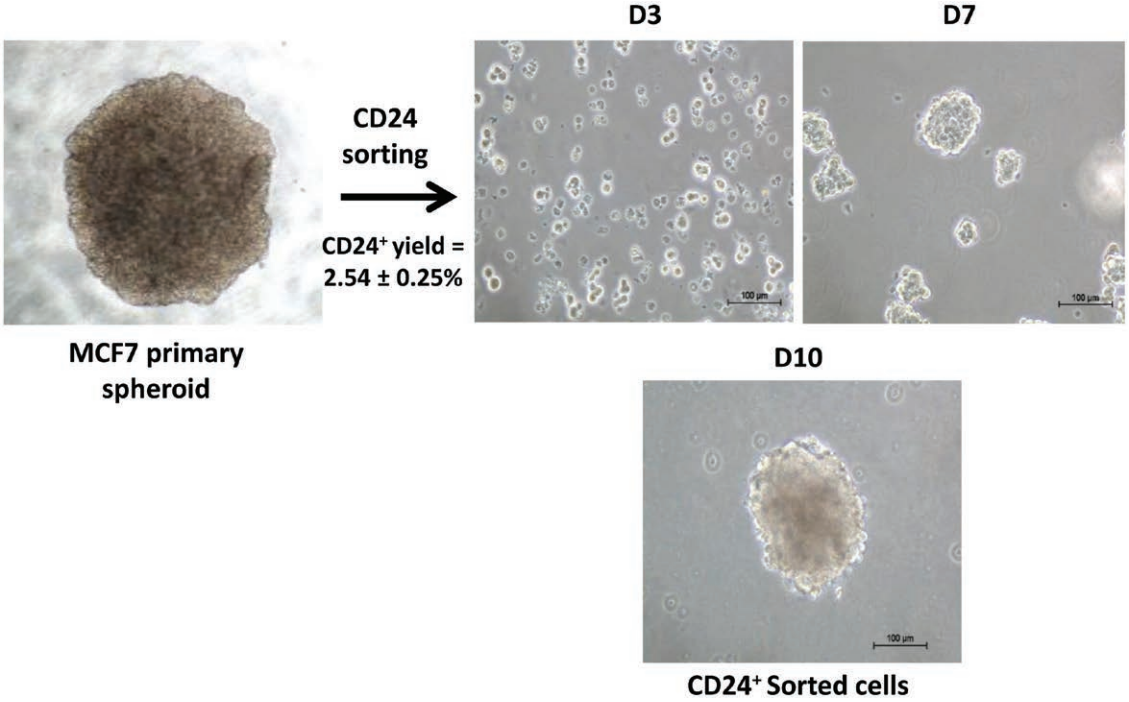

Fig. 1 Spheroid formation efficiency of sorted $CD24^+$ MCF-7 cells at days 3, 7, and 10. MCF-7, Michigan Cancer Foundation-7.

subjected to spheroid formation using serum-free media. Spheroids were able to form on day 7 and reached the size above 100 μm at day 10 (Fig. 1).

3.2. Immunofluorescent observation of CSCs-related markers of CD24⁺ MCF-7 cells

Spheroids generated from sorted CD24⁺ MCF-7 cells were subjected to immunofluorescent microscopic observation after staining with different stem cell–related markers. CD24 was brighter compared with the CD44 markers, whereas Oct4 and Sox2 were negative while the CD49f and Nanog markers were dim in the immunofluorescent staining. On the other hand, the level of ALDH1 was highly expressed as detected with immunofluorescence assay.

3.3. Wound healing, invasion, and migration capacity of CD24⁺ MCF-7 cells

In terms of wound healing assay and invasion, the sorted CD24⁺ MCF-7 cells recorded a delay of wound closure and lower invasion compared with that of the parental MCF-7 cells (Fig. 2 and Fig. 3). No difference was observed for the cell migration between the parental and CD24⁺ MCF-7 cells (Fig. 3).

3.4. Drug resistant of CD24⁺ MCF-7 cells

IC_{50} values of doxorubicin and cisplatin were 5.9 and 2.3 times higher, respectively, for the sorted CD24⁺ MCF-7 cells compared with the parental counterpart (Table 1).

3.4. miRNA expression pattern of CD24⁺ MCF-7 cells

MiRNAs expression profile of CD24⁺ MCF-7 cells was profiled using Illumina small RNA next-generation sequencing. Differential expression between sorted CD24⁺ and parental MCF-7 cells was evaluated using CLC-Genomic Workbench (Qiagen Germantown, MD, USA). A total of 149 miRNAs were differentially expressed with a fold change >2 in CD24⁺ MCF-7 cells (70 downregulated and 79 upregulated). Table 2 shows differentially expressed miRNA with >3 folds. MiR-204, miR-4508, miR-6087, miR-7641, and miR-4492 were the five most upregulated miRNA with a fold change of more than 50. In contrary, miR-1271, miR-181a-2, miR-155, miR-27a, and miR-99a were the five most downregulated miRNA with a fold change of more than 5. In addition, differential expression of five downregulated miRNA (miR-181a, miR-128, let07b, miR-222, and miR-15b) and two upregulated miRNA (miR-34a and miR-30e) were validated using quantitative real-time PCR. The result of quantitative real-time PCR was consistent with the sequencing result (Fig. 4). Sequencing data can be found under GEO accession number GSE95598.

Based on the differentially regulated miRNA, target genes of these significant miRNA and GO for molecular function, biological processes and cellular components were predicted using Database for Annotation, Visualization and Integrated Discovery. The top 10 GOs for each category were shown in Fig. 5. Regulation of transcription, DNA-dependent and signal transduction were

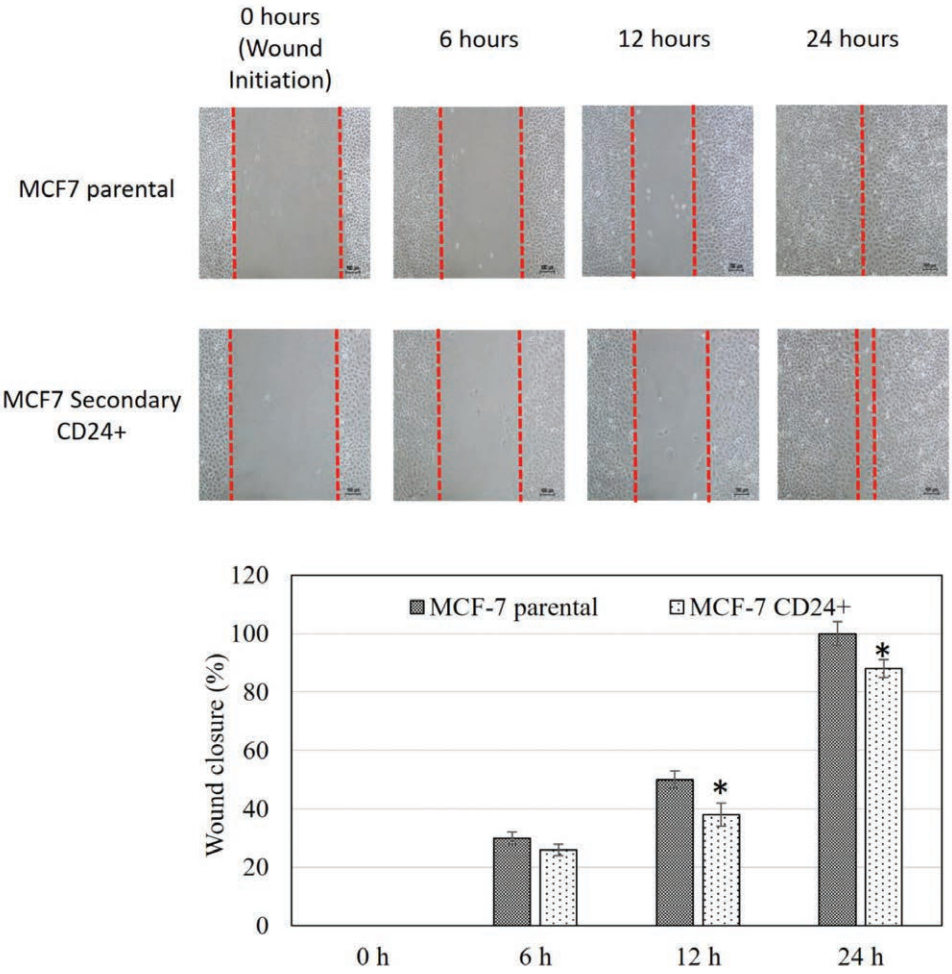

Fig. 2 Wound healing of parental and sorted CD24⁺ MCF-7 cells. All data were expressed as mean ± SDs and *$p < 0.05$ compared with parental cells. Magnification at 10×. MCF-7, Michigan Cancer Foundation-7.

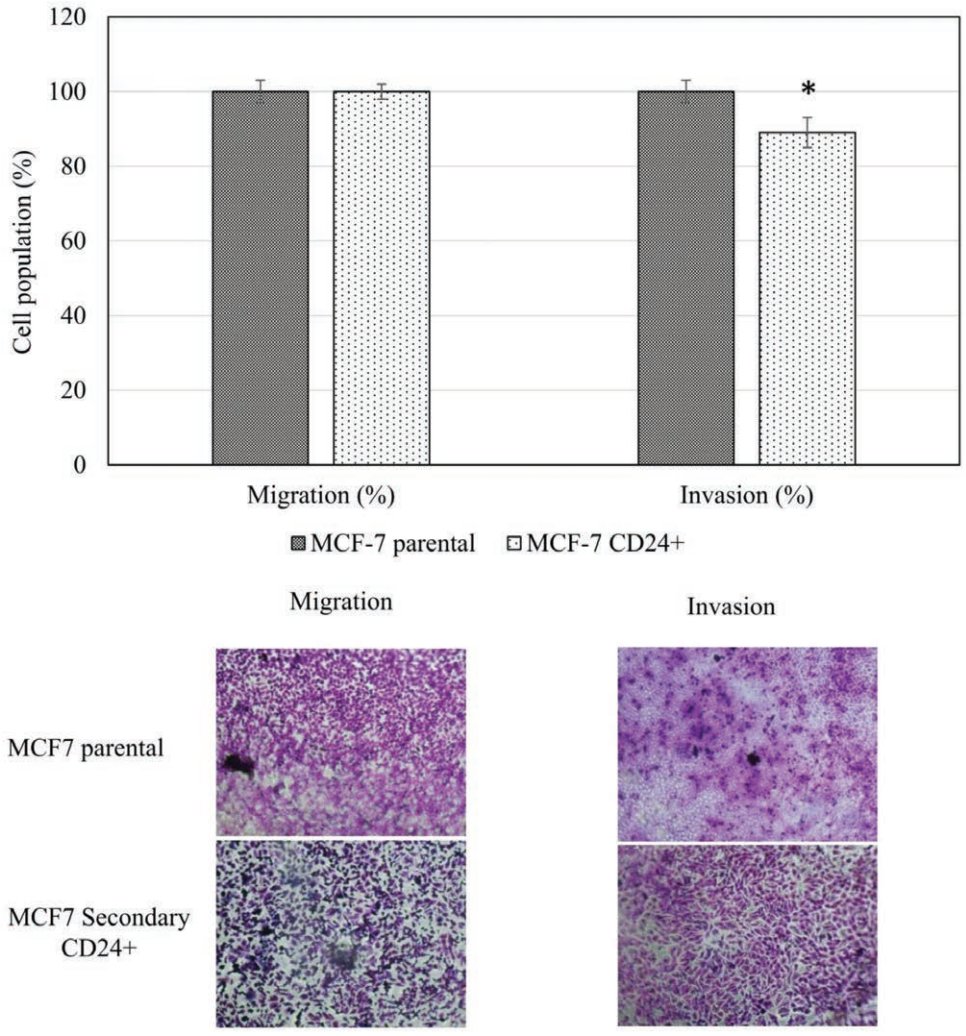

Fig. 3 Migration and invasion capacity of parental and sorted CD24⁺ MCF-7 cells. All data were expressed as mean ± SDs and *$p < 0.05$ compared with parental cells. Magnification at 10×.

Table 1

The IC_{50} value (μM) of doxorubicin and cisplatin in parental and sorted CD24⁺ MCF-7 cells after 96 hours of incubation

	IC_{50} Value (μM)	
	Doxorubicin	Cisplatin
MCF-7 parental cells	0.89 ± 0.26	3.11 ± 0.52
CD24⁺ MCF-7 cells	5.31 ± 2.17[a]	7.35 ± 1.75[a]

IC_{50} = concentration of drug that reduced 50% of cell viability; MCF-7 = Michigan Cancer Foundation-7; MAPK = microtubule associated protein kinase, Wnt = wingless-related integration site; TGF-b = transforming growth factor beta.

[a]$p < 0.05$ compared with MCF-7 parental cells.

the two most highly regulated biological process in GO analysis. In addition, protein binding and metal ion binding were the two most highly regulated molecular function (Fig. 5).

In terms of KEGG pathway analysis, CSCs-related pathways such as Hedgehog signaling pathway, wingless-related integration site (Wnt) signaling pathway, transforming growth factor beta (TGF-β) signaling pathway, and insulin signaling pathway were found downregulated. In addition, microtubule associated protein kinase (MAPK) signaling pathway and the majority of pathways in cancer-related genes were found to be downregulated as well. Pathways that are related to epithelial-like cell states such as adherens junction, tight junction, and focal adhesion were found upregulated (Table 3).

4. DISCUSSION

While studies of breast cancer spheroid mainly focused on $CD44^{+}CD24^{-/dim}$ subpopulation, characteristic and drug response of CD24⁺ subpopulation were somehow neglected.[11–13] In this study, CD24⁺ subpopulation was sorted from primary MCF-7 spheroid and subjected to further characterization and miRNA profiling in comparison with the parental MCF-7 cells. Based on the results, the sorted CD24⁺ possesses good purity (>90%), but the yield (≈2.5%) was lower than the percentage of $CD24^{+}CD44^{-}$ cell population of MCF-7 spheroid detected by flow cytometry in the previous report.[5] The CD24⁺ MCF-7 cells were less efficient in spheroid formation and were generally smaller compared with the parental cells. Spheroid formation assay has been widely used as standard method for characterization of stem cells including CSCs.[14] However, our results indicated that the used of spheroid formation efficiency as the sole characterization method for CSCs may not be sufficient particularly on cancer cell samples which consist of a mixture of subpopulation since as even non-CSC subpopulation was able to form spheroids.

Table 2

Upregulated and downregulated miRNA in sorted CD24⁺ MCF-7 cells when compared with that of the parental MCF-7 cells

MCF-7 CD24⁺ Upregulated miRNA	Fold Changed	*p*	MCF-7 CD24⁺ Downregulated miRNA	Fold Changed	*p*
miR-204	150.82	0.000	miR-1271	−15.15	0.000
miR-4508	98.35	0.000	miR-181a-2	−10.51	0.000
miR-6087	79.26	0.000	miR-155	−7.52	3.33E-06
miR-7641-1/miR-7641-2	52.07	5.647E-12	miR-27a	−5.22	0.000
miR-4492	51.34	0.000	miR-99a	−5.19	6.9E-05
miR-3607	22.66	0.000	miR-219a-1	−5.19	0.000
miR-153-1/miR-153-2	20.25	1.526E-08	miR-301a	−4.84	8.14E-06
miR-499a	20.25	6.301E-05	miR-365a	−4.74	1.6E-07
miR-33a	12.16	0.000	miR-99b	−4.68	0.000
miR-139	10.93	1.11E-15	miR-592	−4.67	8.87E-10
miR-4532	10.74	2.928E-12	miR-92a-1	−4.60	2.99E-14
miR-200b	10.60	0.000	miR-100	−4.56	0.000
miR-1291	10.44	0.000	miR-4286	−4.46	0.000
miR-200a	9.85	0.000	miR-195	−4.44	5.21E-08
miR-142	8.68	0.024	miR-221	−4.43	0.000
miR-410	8.68	4.486E-07	let-7f-1	−4.38	0.000
miR-429	8.25	0.000	miR-148a	−4.24	0.000
miR-1246	8.07	0.000	miR-320b-1/miR-320b-2	−4.13	3.63E-11
miR-362	7.23	8.972E-05	let-7b	−4.08	0.000
miR-708	7.23	8.972E-05	miR-4454	−4.00	0.000
miR-4485	6.94	2.267E-05	miR-184	−3.96	0.000
miR-1296	6.75	0.001	miR-4448	−3.77	5.89E-06
miR-190a	6.27	2.017E-05	miR-222	−3.68	0.000
miR-211	5.79	0.022	miR-30c-1	−3.66	8.24E-13
miR-33b	5.58	0.000	miR-375	−3.64	3.93E-11
miR-196a-2	5.56	0.000	let-7g	−3.63	0.001
miR-545	5.37	3.193E-12	miR-7977	−3.62	0.000
miR-219a-1	5.21	0.001	miR-331	−3.59	0.000
miR-138-2/miR-138-1	4.94	0.000	miR-25	−3.52	0.000
miR-101-1	4.82	0.017	miR-330	−3.51	0.001
miR-450b	4.82	0.001	miR-29b-1	−3.30	6.46E-05
miR-34c	4.73	7.335E-06	let-7d	−3.30	0.000
miR-335	4.34	3.391E-06	miR-128-1	−3.15	0.000
miR-32	4.32	0.000	miR-1468	−3.11	0.000
miR-126	4.12	1.309E-11			
miR-19a	4.10	0.000			
miR-96	4.10	0.000			
miR-30e	3.78	0.000			
miR-29b-1/miR-29b-2	3.71	0.000			
miR-188	3.47	0.028			
miR-3653	3.47	0.028			
miR-449a	3.37	0.000			
miR-885	3.37	5.714E-05			
miR-194-1/miR-194-2	3.35	0.000			
miR-141	3.28	0.000			
miR-3613	3.22	0.000			
miR-3651	3.21	0.0071937			
miR-30a	3.11	0.000			
miR-215	3.04	1.216E-07			

Although the sorted CD24⁺ MCF-7 cells were able to form spheroids, the immunofluorescent results have shown that the stem cell–related markers namely CD44, CD49f, Nanog, Oct4, and Sox2 were either dim or not expressed (Fig. 6), a stark contrast to that of $CD44^{+}CD24^{-}$ which represents the side population of CSCs.[11–13] Moreover, Nanog, Oct4, and Sox2 were three basic transcription factors expressed in both cancer and embryonic stem cells, which maintains their pluripotent and self-renewal characteristics.[15] Unlike the other markers, ALDH1 was found highly expressed in the sorted CD24⁺ MCF-7 cells. Although ALDH was commonly identified as a putative CSCs marker,[10] some studies have also reported that ALDH1 may be highly expressed in other side population of cancer or even normal cells.[1,16] Moreover, concurrent detection of CD49f, ALDH, and $CD44^{+}CD24^{-}$ was more commonly found in the mesenchymal-like cells with multilineage characteristic.[10,17] Furthermore, increasing evidence has shown that CSC promotes cancer progression through epithelial-mesenchymal transition (EMT) which generally results in high cell motility and invasion capacity of the cancer cells.[18,19] On the other hand, dim expression of CD49f and bright level of ALDH suggest that the sorted CD24⁺ MCF-7 cells may possess

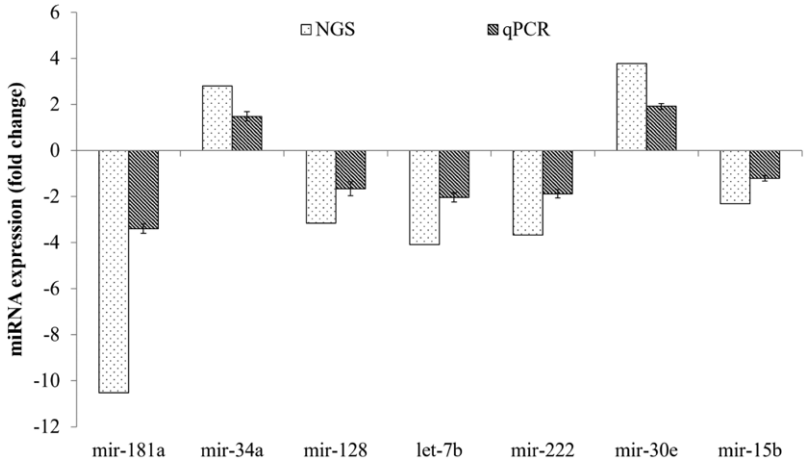

Fig. 4 Quantitative real-time PCR validation of miR-181a, miR-34a, miR-128, let-7b, miR-222, miR-30e, and miR-15b. The results were presented as fold change comparing between sorted $CD24^+$ with the parental MCF-7 cells. All data were expressed as mean ± SDs. PCR, polymerase chain reaction.

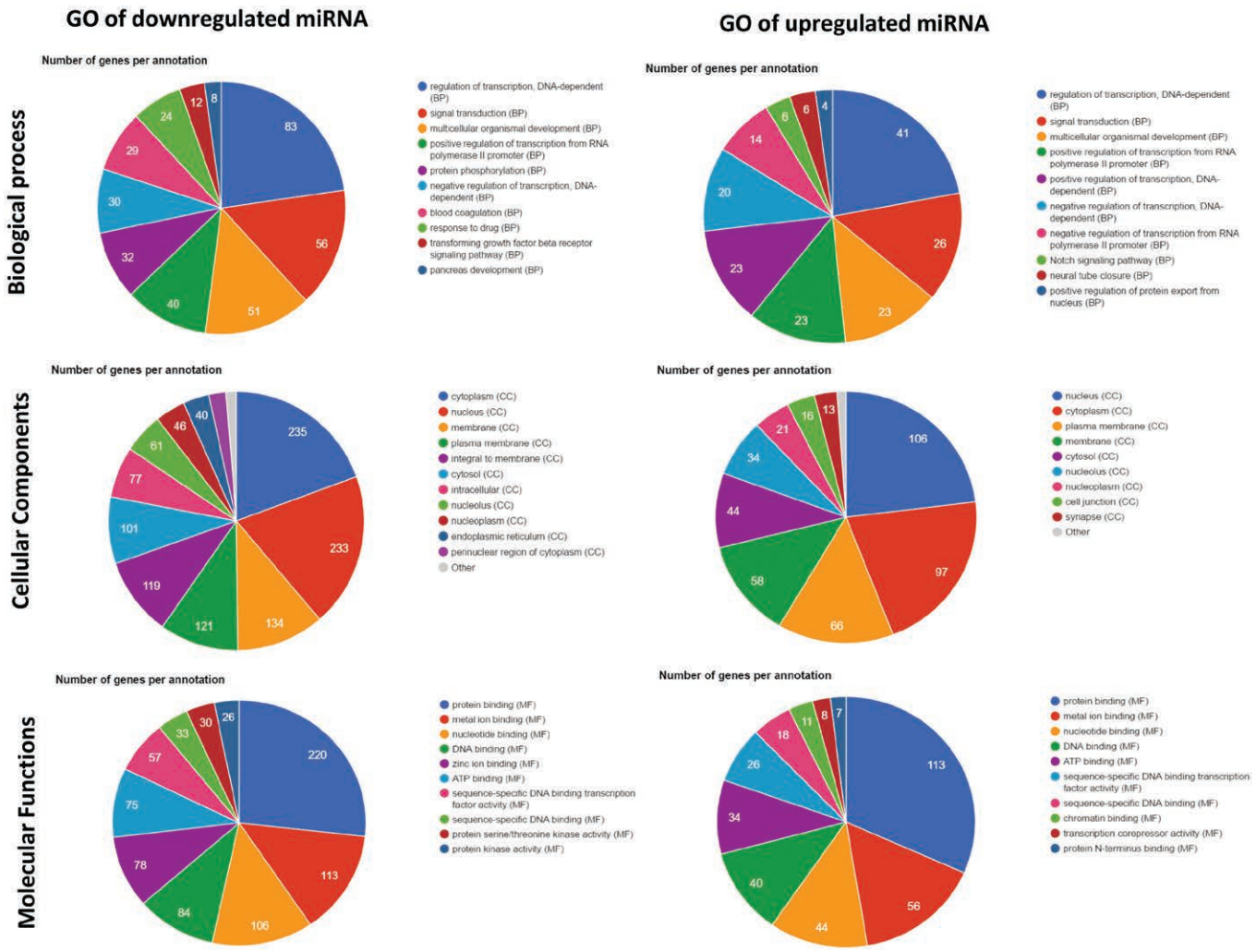

Fig. 5 Top 10 enriched gene ontology (GO) in the up- and downregulated predicted mRNA from the differentially regulated miRNA between sorted $CD24^+$ and the parental MCF-7 cells.

Table 3

The enriched KEGG) pathways of the up- and downregulated predicted genes of the differentially expressed miRNA using DAVID

Downregulated KEGG Pathway	Gene Count	Upregulated KEGG Pathway	Gene Count
(KEGG) 05200: Pathways in cancer	32	(KEGG) 04144: Endocytosis	10
(KEGG) 04144: Endocytosis	17	(KEGG) 04520: Adherens junction	6
(KEGG) 05210: Colorectal cancer	10	(KEGG) 05412: Arrhythmogenic right ventricular cardiomyopathy	5
(KEGG) 04110: Cell cycle	12	(KEGG) 05152: Tuberculosis	7
(KEGG) 04360: Axon guidance	12	(KEGG) 04530: Tight junction	6
(KEGG) 04810: Regulation of actin cytoskeleton	15	(KEGG) 04510: Focal adhesion	7
(KEGG) 04010: MAPK signaling pathway	17	(KEGG) 05200: Pathways in cancer	9
(KEGG) 04722: Neurotrophin signaling pathway	11	(KEGG) 04670: Leukocyte transendothelial migration	5
(KEGG) 04660: T cell receptor signaling pathway	10	(KEGG) 04142: Lysosome	5
(KEGG) 05211: Renal cell carcinoma	8	(KEGG) 04722: Neurotrophin signaling pathway	5
(KEGG) 04340: Hedgehog signaling pathway	7		
(KEGG) 04310: Wnt signaling pathway	11		
(KEGG) 04380: Osteoclast differentiation	10		
(KEGG) 05219: Bladder cancer	6		
(KEGG) 04350: TGF-β signaling pathway	8		
(KEGG) 04910: Insulin signaling pathway	10		

Gene count represent mRNA target by the significantly up- or downregulated miRNA.

DAVID = Database for Annotation, Visualization and Integrated Discovery; KEGG = Kyoto Encyclopedia of Genes and Genomes; MAPK = microtubule associated protein kinase; TGF-β = transforming growth factor beta; Wnt = wingless-related integration site.

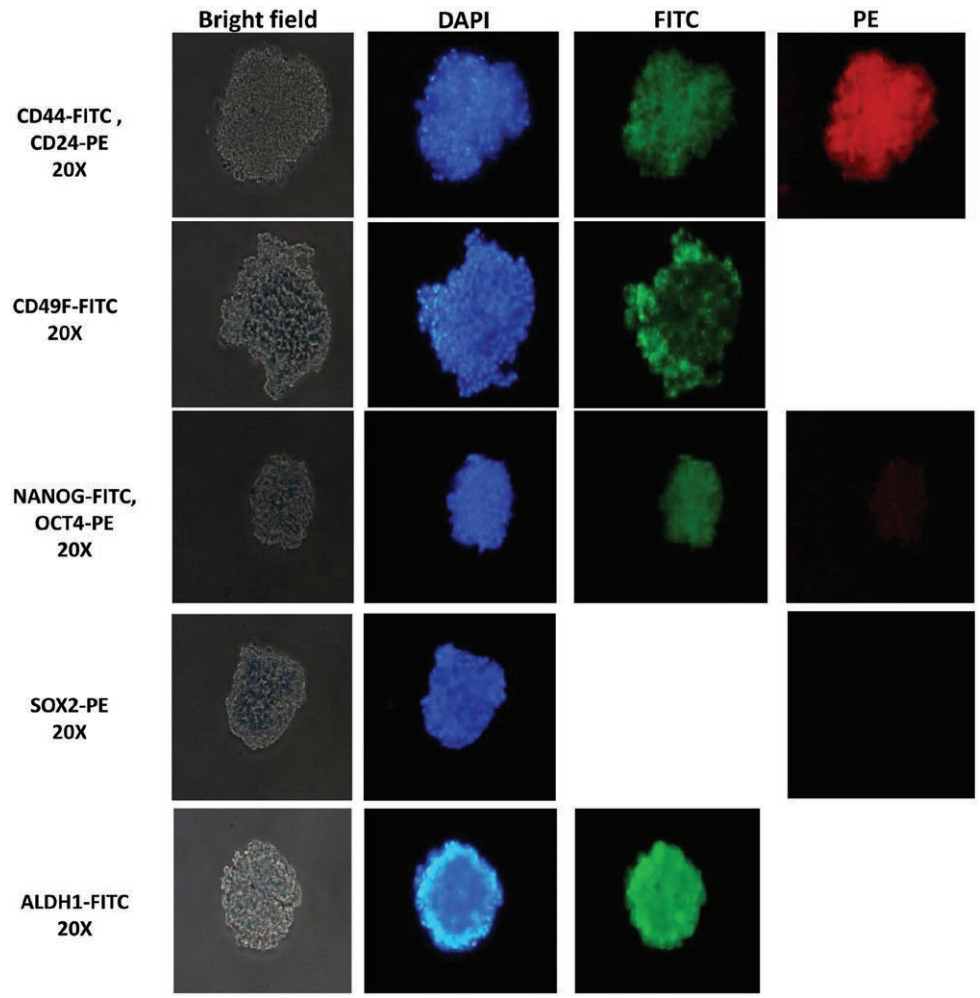

Fig. 6 Immunofluorescent staining of CD44, CD24, CD49f, Nanog, Sox2, Oct4, and ALDH1 on sorted $CD24^+$ MCF-7 cells. DAPI was used for nuclear counterstain. Magnification at 10×. DAPI, 4′,6-diamidino-2-phenylindole; FITC, fluorescein isothiocyanate; PE: phycoerythrin.

epithelial-like features.[10] This idea was supported by the wound healing and invasion assays in which the sorted CD24+ MCF-7 cells were found with a delayed wound healing duration and were less invasive compared with that of the parental MCF-7 cells. Although sorted CD24+ MCF-7 cells were less invasive and not associated with CSC characteristic, resistant against doxorubicin and cisplatin was still exhibited by this side population of cells (Table 1). This phenomenon is in line with the findings from a previous study in which ALDH1 was shown to have contributed to the drug-resistant feature and poor prognosis of breast cancer.[20,21] However, the IC_{50} value of sorted CD24+ MCF-7 cells was still lower than the primary MCF-7 spheroid indicating that the CSC subpopulation with high level of ALDH expression was still more resistant to chemotherapeutic drug treatment.[5]

MiRNA is a class of endogenous noncoding RNA that plays an important role in regulating several cellular and developmental processes by epigenetically regulating gene expression. Abnormal miRNA expression may contribute to various human diseases including cancer and more particularly development of CSCs.[22] For example, miR-200a and miR-200b under miR-200 family were found upregulated in the sorted CD24+ MCF-7 cells (Table 2). MiR-200 family was reported as a tumor suppressor, which inhibited EMT progression and development of CSCs from normal progenitor cells.[23] Moreover, overexpression of miR-204 in CD24+ MCF-7 cells also indicated that this population of cell contributed less to tumor progression as miR-204 was reported as a suppressor of EMT.[24,25] In addition, overexpression of miR-30e and miR34a was able to inhibit self-renewal and EMT of CSCs.[26,27] On the other hand, miR-181a and let-7 which are known to promote stem cell–like features including self-renewal and tumorigenicity in breast cancer were found downregulated in the sorted CD24+ MCF-7 cells.[28,29] To overview the regulation of these significantly regulated miRNA in the sorted CD24+ MCF-7 cells, KEGG pathway analysis was performed. Multiple CSCs-related pathways such as Hedgehog, Wnt, TGF-β, and insulin signaling pathways were found downregulated in the sorted CD24+ MCF-7 cells.[2,30] On the other hand, pathways that were related to reduce EMT such as tight junction and adherens junction were found upregulated.[31] These results indicate that miRNAs play important roles in maintaining non-CSCs characteristic and lower invasiveness of CD24+ side population in MCF-7 spheroid culture. However, further studies to evaluate the expression of EMT and tight junction/adherens junction genes of these sorted cells will provide the much-needed validated data on the potential role of these microRNAs in maintaining the distinct characteristics of the CD24+ sorted MCF-7 populations.

In conclusion, overall CD24+ MCF-7 cells did not possess the common CSC features but had shown higher resistant against the tested chemotherapy drugs namely doxorubicin and cisplatin when compared with the parental cell and were able to generate high levels of ALDH expression. Therefore, the biological characteristics and miRNA profiling of the sorted CD24+ cells described in this study show among others the potential influence of the non–stem cancer cell subpopulation on cancer drug effects and in the dynamic transition of breast CSC phenotypes. However, to counter the limitations of this study, comparative analysis between the microRNA profiling of CD24+ MCF-7 cells with that of the sorted CD44+/CD24− CSC MCF-7 cells and the inclusion of additional CSC markers such as CD133 are to be explored to further validate the indicated microRNAs that could be responsible for the maintenance of the higher drug resistance and ALDH expression of CD24+ MCF-7 cells.

ACKNOWLEDGMENTS

This study was supported by Ministry of Science, Technology and Innovation of Malaysia (MOSTI) for the E-Science Fund (02-02-11-SF0125); Makna grant 2013 (NVHD0001) from Malaysia National Cancer Council Malaysia; Fundamental Research Grant Scheme (FRGS/1/2014/SG05/UNIM/02/1,NFHD0002) from Ministry of Higher Education, Malaysia; and Universiti Tunku Abdul Rahman Research Fund (UTARRF) (A6200/A23) for the financial support.

REFERENCES

1. Gupta Piyush B, Fillmore Christine M, Jiang G, Shapira Sagi D, Tao K, Kuperwasser C, et al. Stochastic state transitions give rise to phenotypic equilibrium in populations of cancer cells. *Cell* 2011;**146**:633–44.
2. Soo JS, Ng CH, Tan SH, Malik RA, Teh YC, Tan BS, et al. Metformin synergizes 5-fluorouracil, epirubicin, and cyclophosphamide (FEC) combination therapy through impairing intracellular ATP production and DNA repair in breast cancer stem cells. *Apoptosis* 2015;**20**:1373–87.
3. Siegel RL, Miller KD, Jemal A. Cancer statistics, 2016. *CA Cancer J Clin* 2016;**66**:7–30.
4. Vincent KM, Findlay SD, Postovit LM. Assessing breast cancer cell lines as tumour models by comparison of mRNA expression profiles. *Breast Cancer Res* 2015;**17**:114.
5. Boo L, Ho WY, Ali NM, Yeap SK, Ky H, Chan KG, et al. MiRNA transcriptome profiling of spheroid-enriched cells with cancer stem cell properties in human breast MCF-7 cell line. *Int J Biol Sci* 2016;**12**:427–45.
6. Ho WY, Yeap SK, Ho CL, Rahim RA, Alitheen NB. Development of multicellular tumor spheroid (MCTS) culture from breast cancer cell and a high throughput screening method using the MTT assay. *Plos One* 2012;**7**:e44640.
7. Li Y, Zhang T, Korkaya H, Liu S, Lee HF, Newman B, et al. Sulforaphane, a dietary component of broccoli/broccoli sprouts, inhibits breast cancer stem cells. *Clin Cancer Res* 2010;**16**:2580–90.
8. Morata-Tarifa C, Jiménez G, García MA, Entrena JM, Griñán-Lisón C, Aguilera M, et al. Low adherent cancer cell subpopulations are enriched in tumorigenic and metastatic epithelial-to-mesenchymal transition-induced cancer stem-like cells. *Sci Rep* 2016;**6**:18772.
9. Meyer MJ, Fleming JM, Ali MA, Pesesky MW, Ginsburg E, Vonderhaar BK. Dynamic regulation of CD24 and the invasive, CD44POSCD24NEG phenotype in breast cancer cell lines. *Breast Cancer Res* 2009;**11**:R82.
10. Liu S, Cong Y, Wang D, Sun Y, Deng L, Liu Y, et al. Breast cancer stem cells transition between epithelial and mesenchymal states reflective of their normal counterparts. *Stem Cell Reports* 2014;**2**:78–91.
11. Sun H, Jia J, Wang X, Ma B, Di L, Song G, et al. CD44+/CD24- breast cancer cells isolated from MCF-7 cultures exhibit enhanced angiogenic properties. *Clin Transl Oncol* 2013;**15**:46–54.
12. Hiscox S, Baruha B, Smith C, Bellerby R, Goddard L, Jordan N, et al. Overexpression of CD44 accompanies acquired tamoxifen resistance in MCF7 cells and augments their sensitivity to the stromal factors, heregulin and hyaluronan. *BMC Cancer* 2012;**12**:458.
13. Nie S, McDermott SP, Deol Y, Tan Z, Wicha MS, Lubman DM. A quantitative proteomics analysis of MCF7 breast cancer stem and progenitor cell populations. *Proteomics* 2015;**15**:3772–83.
14. Shaheen S, Ahmed M, Lorenzi F, Nateri AS. Spheroid-formation (colonosphere) assay for in vitro assessment and expansion of stem cells in colon cancer. *Stem Cell Rev Rep* 2016;**12**:492–9.
15. Liu A, Yu X, Liu S. Pluripotency transcription factors and cancer stem cells: small genes make a big difference. *Chin J Cancer* 2013;**32**:483–7.
16. Adams A, Warner K, Pearson AT, Zhang Z, Kim HS, Mochizuki D, et al. ALDH/CD44 identifies uniquely tumorigenic cancer stem cells in salivary gland mucoepidermoid carcinomas. *Oncotarget* 2015;**6**:26633–50.
17. Hass R, Kasper C, Böhm S, Jacobs R. Different populations and sources of human mesenchymal stem cells (MSC): a comparison of adult and neonatal tissue-derived MSC. *Cell Commun Signal* 2011;**9**:12.
18. Sheridan C, Kishimoto H, Fuchs RK, Mehrotra S, Bhat-Nakshatri P, Turner CH, et al. CD44+/CD24- breast cancer cells exhibit enhanced invasive properties: an early step necessary for metastasis. *Breast Cancer Res* 2006;**8**:R59.
19. Yan W, Chen Y, Yao Y, Zhang H, Wang T. Increased invasion and tumorigenicity capacity of CD44+/CD24- breast cancer MCF7 cells in vitro and in nude mice. *Cancer Cell Int* 2013;**13**:62.

20. Keysar SB, Jimeno A. More than markers: biological significance of cancer stem cell-defining molecules. *Mol Cancer Ther* 2010;**9**:2450–7.
21. Tan EY, Thike AA, Tan PH; Breast Surgical Team at Outram. ALDH1 expression is enriched in breast cancers arising in young women but does not predict outcome. *Br J Cancer* 2013;**109**:109–13.
22. Takahashi RU, Miyazaki H, Ochiya T. The role of microRNAs in the regulation of cancer stem cells. *Front Genet* 2014;**4**:295.
23. Feng X, Wang Z, Fillmore R, Xi Y. Mir-200, a new star miRNA in human cancer. *Cancer Lett* 2014;**344**:166–73.
24. Li W, Jin X, Zhang Q, Zhang G, Deng X, Ma L. Decreased expression of miR-204 is associated with poor prognosis in patients with breast cancer. *Int J Clin Exp Pathol* 2014;**7**:3287–92.
25. Qiu YH, Wei YP, Shen NJ, Wang ZC, Kan T, Yu WL, et al. MiR-204 inhibits epithelial to mesenchymal transition by targeting slug in intrahepatic cholangiocarcinoma cells. *Cell Physiol Biochem* 2013;**32**:1331–41.
26. Liu C, Kelnar K, Liu B, Chen X, Calhoun-Davis T, Li H, et al. The microRNA miR-34a inhibits prostate cancer stem cells and metastasis by directly repressing CD44. *Nat Med* 2011;**17**:211–5.
27. Yu F, Deng H, Yao H, Liu Q, Su F, Song E. MiR-30 reduction maintains self-renewal and inhibits apoptosis in breast tumor-initiating cells. *Oncogene* 2010;**29**:4194–204.
28. Wang Y, Yu Y, Tsuyada A, Ren X, Wu X, Stubblefield K, et al. Transforming growth factor-β regulates the sphere-initiating stem cell-like feature in breast cancer through miRNA-181 and ATM. *Oncogene* 2011;**30**:1470–80.
29. Yu F, Yao H, Zhu P, Zhang X, Pan Q, Gong C, et al. Let-7 regulates self renewal and tumorigenicity of breast cancer cells. *Cell* 2007;**131**:1109–23.
30. Czerwinska P, Kaminska B. Regulation of breast cancer stem cell features. *Contemp Oncol (Pozn)* 2015;**19**:A7–A15.
31. Knights AJ, Funnell APW, Crossley M, Pearson RCM. Holding tight: cell junctions and cancer spread. *Trends Cancer* 2012;**8**:61–9.